EW-7197, an activin-like kinase 5 inhibitor, suppresses granulation tissue after stent placement in rat esophagus

Eun Jung Jun, PhD,[1,*] Jung-Hoon Park, PhD,[1,2,*] Jiaywei Tsauo, MD,[1] Su-Geun Yang, PhD,[3] Dae-Kee Kim, PhD,[4] Kun Yung Kim, MD,[1] Min Tae Kim, MS,[1] Sung-Hwan Yoon, BS,[1] Young Je Lim, BS,[1] Ho-Young Song, MD[1]

Seoul, Republic of Korea

Background and Aims: Self-expanding metallic stent (SEMS) placement is a well-established method for treating malignant esophageal strictures; however, this procedure has not gained widespread acceptance for treating benign esophageal strictures because of granulation tissue formation. The aim of the present study was to investigate whether EW-7197, a novel per-oral transforming growth factor-β type I receptor kinase inhibitor, suppressed granulation tissue formation after SEMS placement in the rat esophagus.

Methods: Sixty rats underwent SEMS placement and were randomly divided into 4 groups. Group A (n = 20) received vehicle-treated control for 4 weeks. Group B (n = 20) received 20 mg/kg/day EW-7197 for 4 weeks. Group C (n = 10) received 20 mg/kg/day EW-7197 for 4 weeks followed by vehicle-treated control for 4 weeks. Group D (n = 10) received 20 mg/kg/day EW-7197 for 8 weeks.

Results: SEMS placement was technically successful in all rats. Eleven rats, however, were excluded because of stent migration (n = 9) and procedure-related death (n = 2). The luminal diameter in group A was significantly smaller than those in groups B, C, and D (all $P < .001$). The percentage of granulation tissue area, number of epithelial layers, thickness of submucosal fibrosis, percentage of connective tissue area, and degree of collagen deposition were significantly higher in group A than in groups B, C, and D (all $P < .001$); however, there were no significant differences among groups B, C, and D. EW-7197 decreased the expression levels of phospho-Smad 3, N-cadherin, fibronectin, α-smooth muscle actin, and transforming growth factor-β1 and increased the expression level of E-cadherin (all $P < .01$).

Conclusions: EW-7197 suppressed granulation tissue formation after SEMS placement in the rat esophagus.

Abbreviations: ALK5, activin-like kinase 5; ECM, extracellular matrix; EMT, epithelial mesenchymal transition; EW-7197, N-[[4-([1,2,4]triazolo[1,5-a]pyridin-6-yl)-5-(6-methylpyridin-2-yl)-1H-imidazol-2-yl]methyl]-2-fluoroaniline; SEMS, self-expanding metallic stent; TGF-β, transforming growth factor β.

DISCLOSURE: *All authors disclosed no financial relationships relevant to this publication. Research support for this study (S-G Yang, H-Y Song) was provided by the Basic Science Research Program through the National Research Foundation of Korea funded by the Ministry of Science, ICT, and Future Planning (NRF-2014R1A2A2A04006562).*

*Drs Jun and Park contributed equally to this article.

Use your mobile device to scan this QR code and watch the author interview. Download a free QR code scanner by searching "QR Scanner" in your mobile device's app store.

0016-5107/$36.00
http://dx.doi.org/10.1016/j.gie.2017.01.013

Received September 5, 2016. Accepted January 10, 2017.

Current affiliations: Department of Radiology and Research Institute of Radiology (1), Biomedical Engineering Research Center (2), Asan Medical Center, University of Ulsan College of Medicine, Seoul, Republic of Korea; Department of New Drug Development and NCEED, School of Medicine, Inha University, Incheon, Republic of Korea (3), Graduate School of Pharmaceutical Sciences, College of Pharmacy, Ewha Women's University, Seoul, Republic of Korea (4).

Reprint requests: Ho-Young Song, MD, PhD, Department of Radiology, Asan Medical Center, University of Ulsan College of Medicine, 88, Olymic-ro 43-gil, Songpa-gu, Seoul, 138-736, Republic of Korea.

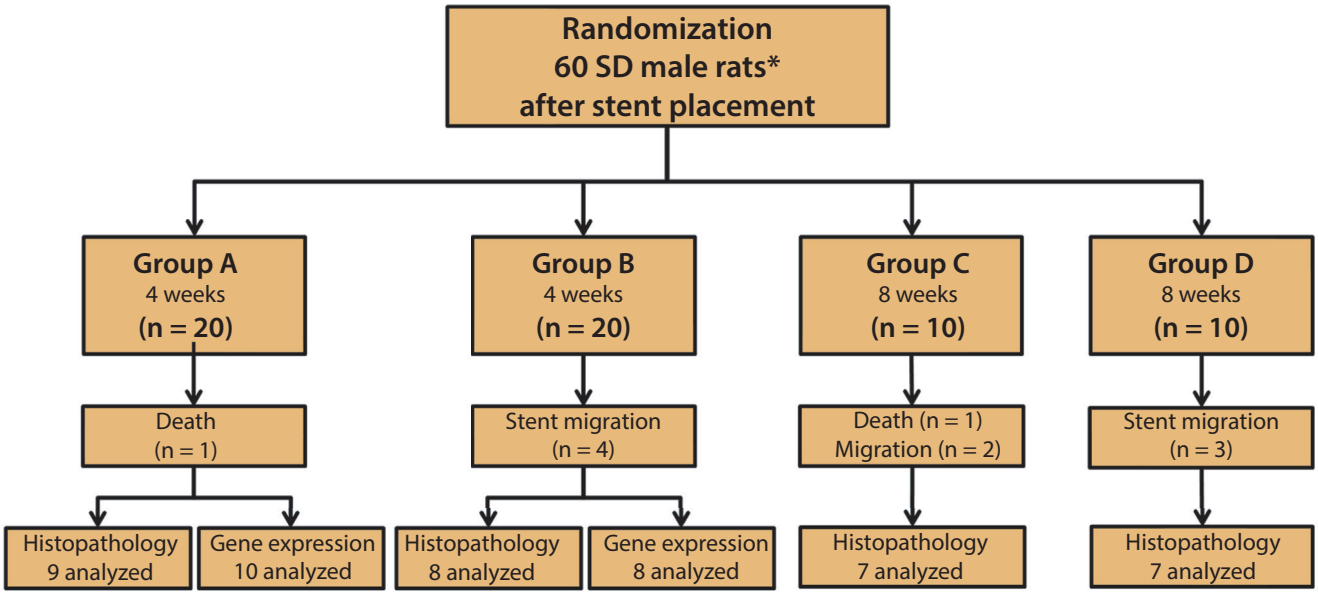

Figure 1. Flow diagram and study design showing the randomization process and follow-up. *SD*, Sprague-Dawley.

Self-expandable metallic stent (SEMS) placement is a well-established method for the treatment of malignant esophageal strictures.[1-4] However, placement of uncovered SEMSs is considered relatively contraindicated for treating benign esophageal strictures because of high risk of granulation tissue formation through the stent mesh framework.[5,6] To solve this problem, retrievable covered SEMSs were developed. Although the covering membrane of these stents could prevent granulation tissue formation through the stent mesh framework, it significantly increases the possibility of stent migration (25%-64%).[5-8] Moreover, granulation tissue formation can occur at both ends of the stent, which leads to recurrence and increases the technical difficulty of stent removal (17%-41%).[5-8]

Granulation tissue formation occurs as an excessive proliferative response to mechanical injury caused by the stent. Activation of the transforming growth factor β (TGF-β) signaling pathway is implicated in angiogenesis, production, and remodeling of the extracellular matrix (ECM) and proliferation of epithelial cells and fibroblasts that leads to stent restenosis.[9,10] TGF-β1 is a member of the TGF-β superfamily that controls processes such as proliferation and differentiation of many cell types.[11,12] Activin-like kinase 5 (ALK5) is a TGF-β1 receptor that phosphorylates SMAD3 and triggers many cellular processes, which are involved in granulation tissue formation, including ECM synthesis and the epithelial mesenchymal transition (EMT).[13-15]

EW-7197 (*N*-[[4-([1,2,4]triazolo[1,5-a]pyridin-6-yl)-5-(6-methylpyridin-2-yl)-1H-imidazol-2-yl]methyl]-2-fluoroaniline) is a novel per-oral TGF-β type I receptor kinase inhibitor. This drug is rapidly absorbed after oral administration and has high selectivity against other kinases and minimal toxicity in animals.[16-18] We hypothesized that EW-7197 might prevent granulation tissue formation after SEMS placement by inhibiting TGF-β1/SMAD3-induced ECM and EMT. The purpose of this study was to investigate whether EW-7197 suppressed granulation tissue formation after SEMS placement in the rat esophagus.

METHODS

This study was approved by the Institutional Animal Care and Use Committee of our institution and conformed to U.S. National Institutes of Health guidelines for humane handling of laboratory animals. The number of animals used to assess the hypothesized difference in granulation tissue formation after stent placement with and without EW-7197 had been calculated prospectively. The mean luminal diameter of the stented esophagus at 4 weeks after stent placement in the rat esophageal model was expected to be around 3.5 mm with a standard deviation of .8 mm based on results of our pilot study (unpublished data). We hypothesized that this diameter would be increased by at least 1 mm in luminal diameter of the stented esophagus with administration of 20 mg/kg EW-7197. We calculated that a total of 40 animals (10 per group) would be required to detect this difference between groups, with an alpha level of .05 and a beta level of .80.

After SEMS placement, 60 Sprague-Dawley rats (300-350 g; Orient Bio, Seongnam, Korea) were randomly distributed into 4 groups using computer-generated random numbers as follows (Fig. 1). Group A (n = 20) received .3 mL of artificial gastric juice by gavage once daily for 4 weeks. Group B (n = 20) received a solution of 20 mg/kg EW-7197 dissolved in .3 mL of

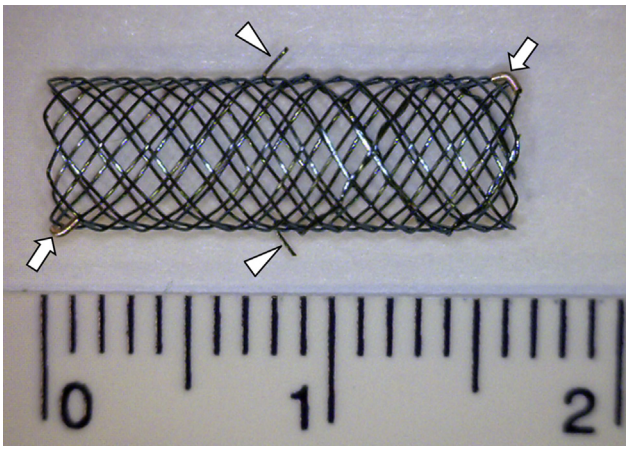

Figure 2. A self-expandable metallic stent. Gold markers were attached to either end of the stent (*arrows*). Two barbs are located in the center of the stent (*arrowheads*).

artificial gastric fluid by gavage once daily for 4 weeks. To evaluate the rebound effect of EW-7197, 2 additional groups were included. Group C (n = 10) received a solution of 20 mg/kg EW-7197 dissolved in .3 mL of artificial gastric fluid by gavage once daily for 4 weeks followed by .3 mL of artificial gastric fluid by gavage once daily for 4 weeks. Group D (n = 10) received a solution of 20 mg/kg EW-7197 dissolved in .3 mL of artificial gastric fluid by gavage once daily for 8 weeks. EW-7197 was provided by the Laboratory of Medicinal Chemistry, College of Pharmacy, Ewha Womans University, Seoul, Korea.

All rats were supplied with food and water ad libitum and were maintained at 22 ± 2°C. The body weights of the rats were measured weekly until they were killed. Groups A and B and groups C and D were killed 4 and 8 weeks after stent placement, respectively. All rats were killed by administrating inhalable pure carbon dioxide. Histologic examination was performed in all groups, and, additionally, Western blot analysis was performed in groups A and B.

Stent construction and placement

The SEMS was knitted from a single thread of .127-mm-thick nitinol wire filament (Fig. 2). The stent was 5 mm in diameter and 15 mm in length. Two barbs were attached to the middle of the stent to prevent migration. Two radiopaque makers at each end of the stent facilitated precise placement. The size of the stent was chosen according to a published study (Taewoong Medicals, Seoul, Korea).[19] Anesthesia was induced by intramuscular injection of 50 mg/kg zolazepam and 50 mg/kg tiletamine (Zoletil 50; Virbac, Carros, France) and 10 mg/kg xylazine (Rompun; Bayer HealthCare, Leverkusen, Germany). A .014-inch guidewire (Transcend; Boston Scientific, Watertown, Mass) was inserted through the mouth and negotiated into the stomach under fluoroscopic guidance, and a 6F sheath (constructed in-house) was advanced over the guidewire into the lower esophagus. The guidewire was removed with the sheath left in place, and a compressed stent was loaded into the sheath. The stent was deployed at the level of the mid-thoracic esophagus under continuous fluoroscopic monitoring. After the procedure, an esophagography was performed to verify the position and patency of the stent.

Esophagographic examination

The rats in each group underwent follow-up esophagography using contrast medium (Omnipaque 300; General Electric Healthcare Company, Shanghai, China) immediately before they were killed. The stented esophagus was divided into proximal, middle, and distal segments. The luminal diameter of each segment was measured on each esophagogram using Photoshop software (version 6.0; Adobe Systems, Palo Alto, Calif). The analyses of the esophagographic findings were accessed on the basis of the consensus of 3 observers blinded to group assignment.

Histologic examination

Surgical exploration of the esophagus and stomach was followed by gross examination to evaluate the degree of granulation tissue formation and to determine possible esophageal injury after stent placement. The stented esophagus of each of 10 rats from each group was sectioned transversely at the proximal and distal regions. Tissue samples were fixed in 10% neutral buffered formalin for 24 hours, which was then embedded in paraffin and sectioned. The slides were stained with hematoxylin and eosin and Masson's trichrome.

Histologic evaluation using hematoxylin and eosin included determining the degree of submucosal inflammatory cell infiltration, the number of epithelial layers, the thickness of submucosal fibrosis, and the granulation tissue–related percentage of the esophageal cross-sectional area of stenosis = 100 × (1 − [stenotic stented area/original stented area]). The degree of inflammatory cell infiltration was subjectively determined according to the distribution and density of the inflammatory cells (graded as 1, mild; 2, mild to moderate; 3, moderate; 4, moderate to severe; and 5, severe). The average values of the number of epithelial layers, thickness of submucosal fibrosis, and degree of inflammatory cell infiltration represented the average value of 8 points around the circumference.[19-21]

The degree of collagen deposition and the percentage of connective tissue area were determined using Masson's trichrome–stained sections. The connective tissue (collagen) area = 100 × (1 − [connective area/original area]). The extent of collagen deposition was subjectively determined, where 1 indicated mild, 2 mild to moderate, 3 moderate, 4 moderate to severe, and 5 severe.

Histologic analysis of the esophagus was performed using a BX51 microscope (Olympus, Tokyo, Japan).

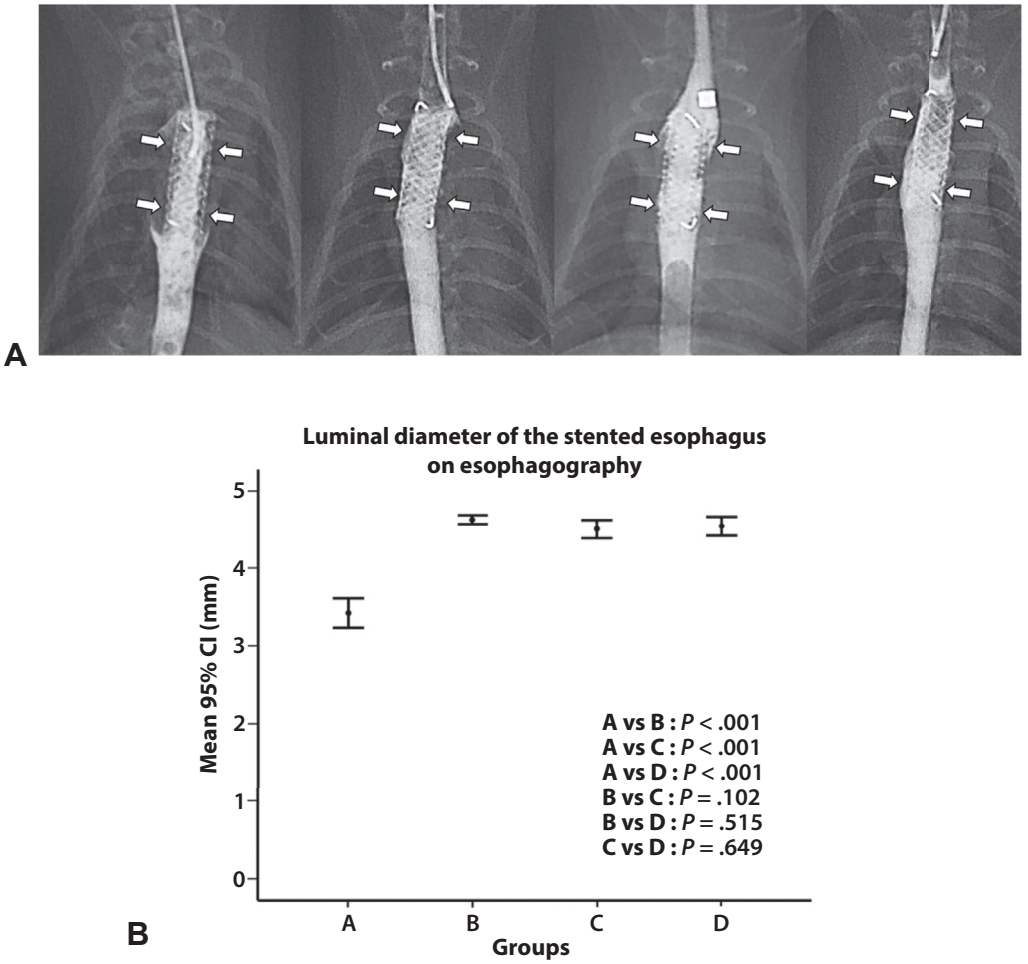

Figure 3. Esophagographic findings. **A,** Representative esophagographic images. From left to right, group A, group B, group C, and group D. Follow-up esophagography performed 4 weeks after stent placement shows filling defects (*arrows*) caused by granulation tissue formation in group A and relatively good patency of the stent (*arrows*) with no definite irregularities in groups B, C, and D. **B,** The mean overall luminal diameter of the stented esophagus. *CI*, Confidence interval.

Image-Pro Plus software (Media Cybernetics, Silver Spring, Md) was used for measurements. The analyses of the histologic findings were accessed on the basis of the consensus of 3 observers blinded to group assignment.

Western blot analysis

We collected the stented esophagi of 10 and 8 rats in groups A and B, respectively. Eight age-matched healthy Sprague-Dawley male rats (Orient Bio) maintained under the same conditions were used for presenting normal values of the esophagus. The antibodies used were as follows: Smad3 (1:1000; Cell Signaling Technology [CST], Danvers, Mass), phospho-Smad 3 (1:1000; CST), E-cadherin (1:1000; CST), N-cadherin (1:1000; CST), α-smooth muscle actin (1:300; Abcam, Cambridge, UK), fibronectin (1:500; Abcam), TGF-β (1:1000; CST), and β-actin (1:1000; Sigma-Aldrich, Louis, Mo). The membranes were incubated in secondary antibodies (1:1000; Jackson ImmunoResearch Laboratories, West Grove, Pa) conjugated to horseradish peroxidase. Target proteins were detected using ECL Western blotting detection reagents (Amersham Biosciences, Little Chalfont, Buckinghamshire, UK), and antigen–antibody complexes were visualized using an Ez-Capture MG software (ATTO Corporation, Tokyo, Japan). CS analyzer software (ATTO Corporation) was used to quantify the bands, and data are expressed as the ratio of band intensity to that of β-actin.

Statistical analysis

Data are expressed as the mean ± standard deviation. The differences between the groups were analyzed using the Kruskal-Wallis or Mann-Whitney U test, as appropriate. A $P < .05$ was considered statistically significant. For $P < .05$ a Bonferroni-corrected Mann-Whitney U test was used to detect the group causing differences ($P < .008$ as statistically significant). Statistical analyses were performed using SPSS software (version 22.0; SPSS, IBM, Chicago, Ill).

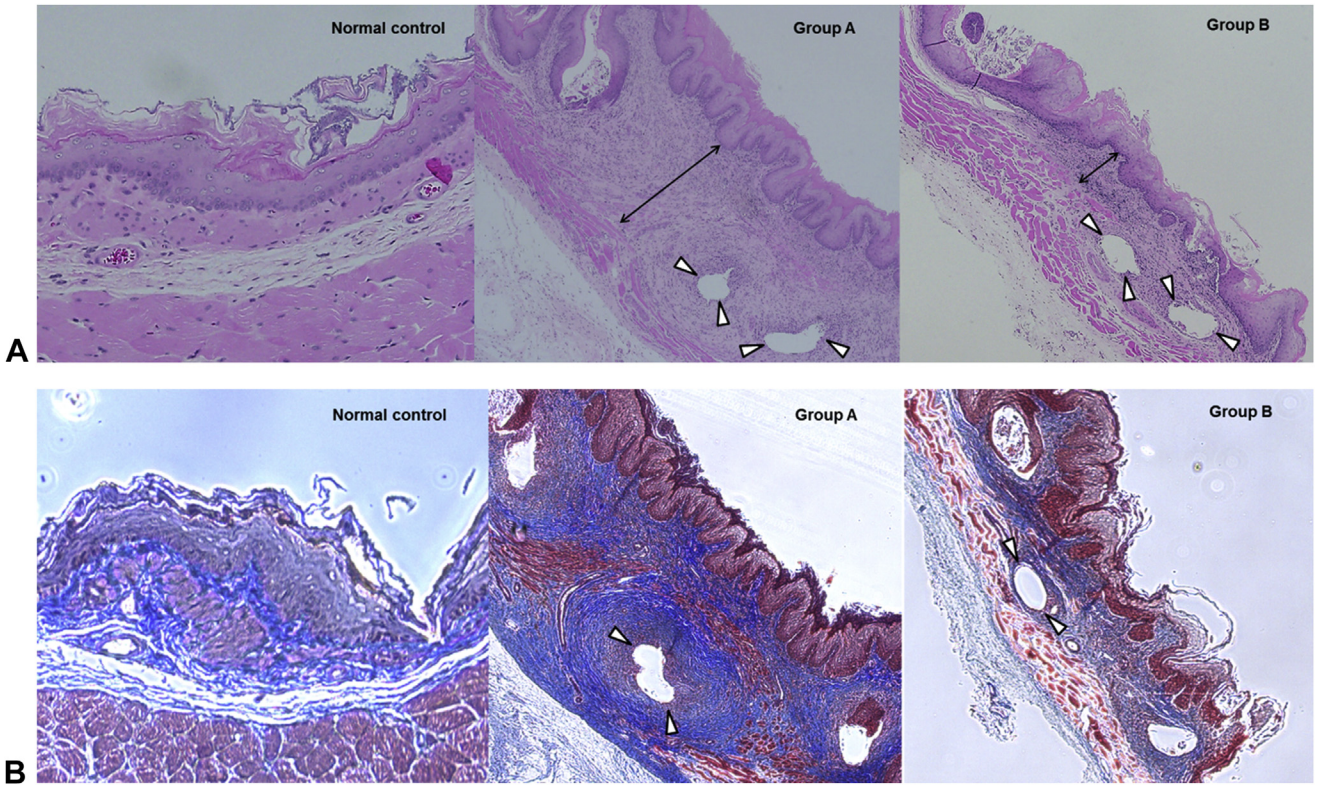

Figure 4. Representative microscopic images. **A,** Microscopic images (H&E, orig. mag. ×10) show significantly smaller thickness of submucosal fibrosis (*black arrows*) in group B than in group A (*arrowheads* indicate stent struts). **B,** Masson's trichrome staining images show relatively less connective tissue area in group B than in group A (*arrowheads* indicate stent struts).

RESULTS

Stent placement was technically successful in all 60 rats. Two rats (3.3%) died 9 and 11 days, respectively, after stent placement because of hematemesis caused by the barbs attached the stent (one in group A and one in group C, respectively). Stent migration occurred in 9 rats (1, 4, 2, and 2 in groups A, B, C, and D, respectively). The 11 rats with stent migration and procedure-related death were excluded from this study. The remaining 49 (81.6%) rats survived until the end of the study with no stent-related adverse events. No adverse events related to EW-7197 administration were observed in any rat. There were no significant differences in body weights between the groups at 4 weeks (450 ± 32.5 g vs 445 ± 35.1 g; $P = .712$) and 8 weeks (497 ± 25.5 g vs 496 g ± 23.7; $P = .368$).

Esophagographic findings

Numeric mean values in the 4 groups were significantly different ($P < .001$, Kruskal-Wallis test). The mean overall luminal diameter of the stented esophagus in group A was significantly smaller than those in groups B, C, and D (3.42 ± .37 mm vs 4.63 ± .13 mm, 4.50 ± .28 mm, and 4.54 ± .29 mm; $P < .001$, $P < .001$, and $P < .001$, respectively). The mean overall luminal diameters were not significantly different among groups B, C, and D (B vs C, $P = .122$; B vs D, $P = .281$; and C vs D, $P = .636$) (Fig. 3).

Histologic findings

Histologic findings are shown in Figures 4 and 5. The mean percentage of granulation tissue area, the mean number of epithelial layers, the mean thickness of submucosal fibrosis, the percentage of connective tissue area, and the degree of collagen deposition were significantly different between the vehicle-treated control group and all 3 drug-treated groups (all variables; $P < .001$, Kruskal-Wallis test). The percentage of granulation tissue area was significantly higher in group A than in groups B, C, and D (56.37% ± 12.22% vs 26.59% ± 7.04%, 31.34% ± 10.79%, and 29.93% ± 9.84%; $P < .001$, $P < .001$, and $P < .001$, respectively). Furthermore, the number of epithelial layers (4.81 ± .78 vs 2.88 ± .56, 3.19 ± .84, and 2.93 ± .69; $P < .001$, $P < .001$, and $P < .001$, respectively) and thickness of submucosal fibrosis (.73 ± .19 mm vs .27 ± .11 mm, .34 ± .12 mm, and .30 ± .11 mm; $P < .001$, $P < .001$, and $P < .001$, respectively) were significantly higher in group A than in groups B, C, and D. However, there were no statistically significant differences among drug-treated groups in the percentage of granulation tissue area (B vs C, $P = .187$; B vs D, $P = .305$; and C vs D, $P = .691$), number of epithelial

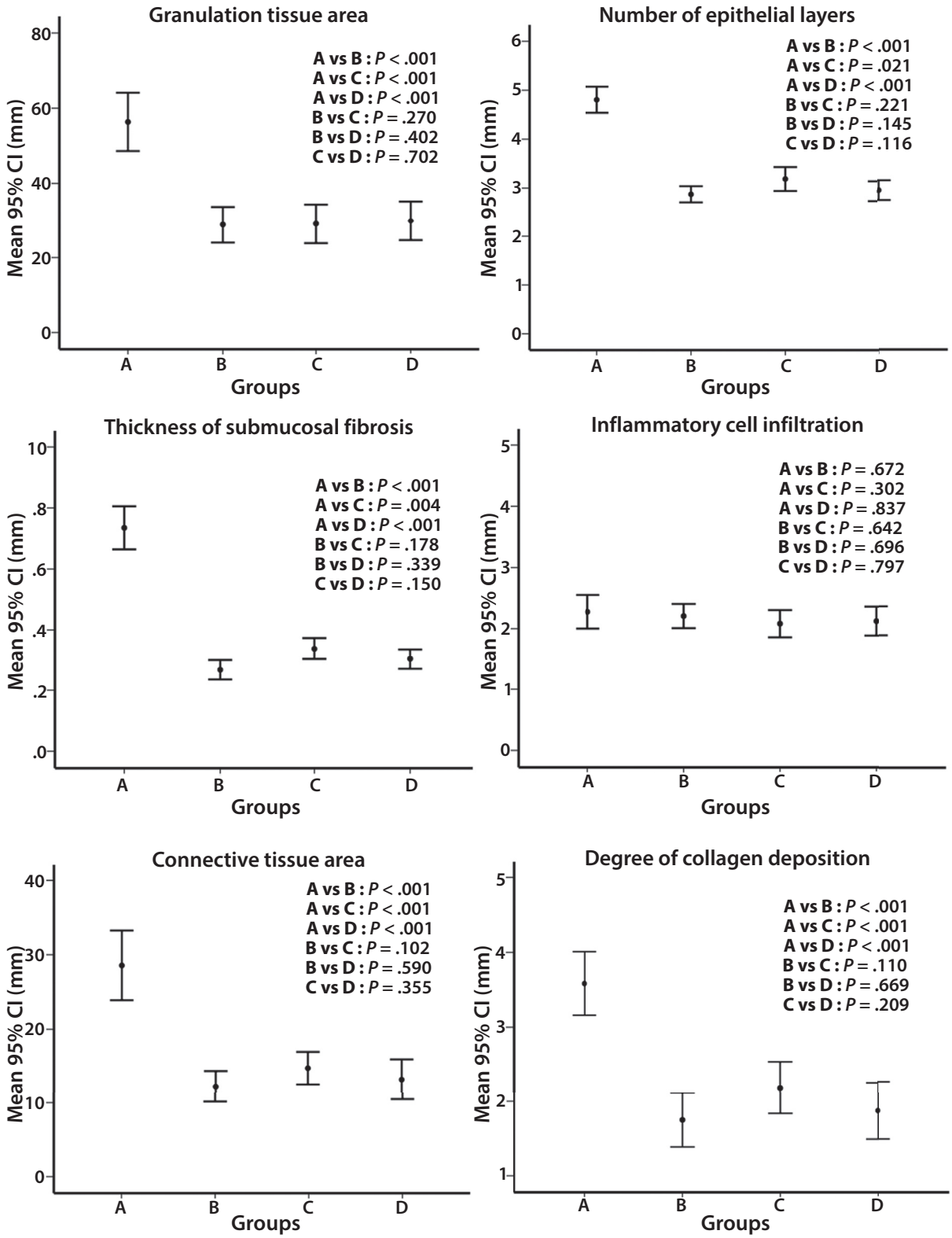

Figure 5. Histopathologic results of the stented esophagus 4 and 8 weeks after stent placement in groups A, B, C, and D. *CI*, Confidence interval.

layers (B vs C, $P = .097$; B vs D, $P = .674$; and C vs D, $P = .194$), and thickness of submucosal fibrosis (B vs C, $P = .178$; B vs D, $P = .183$; and C vs D, $P = .196$).

The density grade of inflammatory cell infiltration was not significantly different among 4 groups (A, 2.28 ± .81; B, 2.21 ± .68; C, 2.13 ± .82; and D, 2.08 ± .76;

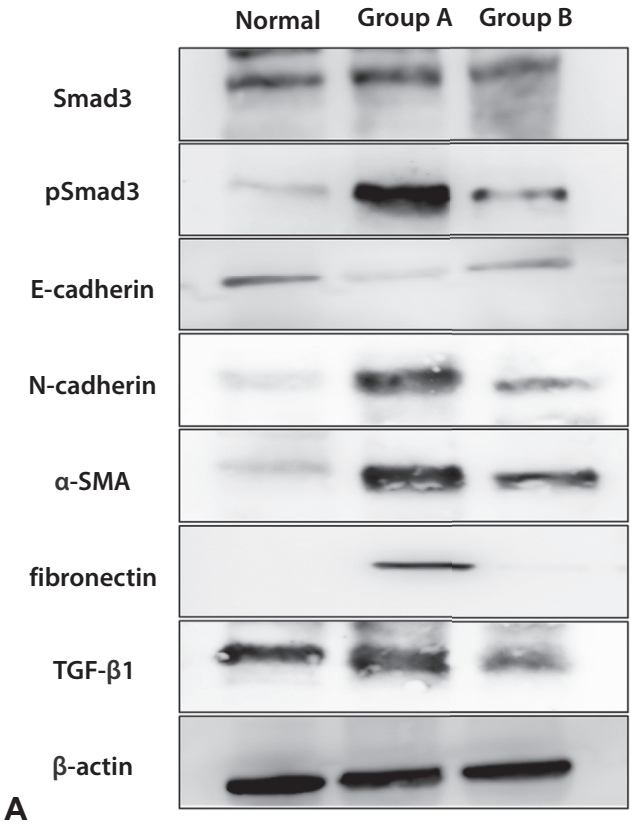

Figure 6. Expression levels of Smad3, phospho-Smad 3 (pSmad3), E-cadherin, N-cadherin, α-smooth muscle actin (SMA), fibronectin, and transforming growth factor (TGF)-β1. **A,** Representative protein expression levels. **B,** Relative fold induction of protein expression levels. β-Actin was used as a reference.

$P = .662$, Kruskal-Wallis test). The percentage of connective tissue area (28.56% ± 7.38% vs 12.26% ± 3.93%, 14.75% ± 4.11%, and 13.21% ± 5.11%; $P < .001$, $P < .001$, and $P < .001$, respectively) and the degree of collagen deposition (3.58 ± .67 vs 1.75 ± .68, 2.18 ± .65, and 1.88 ± .72; $P < .001$, $P < .001$, and $P < .001$, respectively) were significantly higher in group A than in groups B, C, and D. There were no statistically significant differences among drug-treated groups (B vs C, $P = .166$; B vs D, $P = .601$; and C vs D, $P = .388$) in the percentage of connective tissue area indicated by the degree of collagen deposition (B vs C, $P = .075$; B vs D, $P = .201$; and C vs D, $P = .607$).

Western blot findings

Western blot findings are presented in Figure 6. The levels of phospho-Smad 3, N-cadherin, α-smooth muscle actin, fibronectin, and TGF-β1 significantly increased in group A versus the normal group ($P = .001$, .002, .001, .001, and .001, respectively), whereas that of E-cadherin significantly decreased in group A compared with the normal group ($P = .003$) and those of Smad3 remained the same in group A and the normal group. The level of phospho-Smad 3 was lower in group B than in group A ($P = .027$), and there was no difference in the levels of Smad3 between them ($P = .916$). Group B expressed lower levels of N-cadherin, α-smooth muscle actin, fibronectin, and TGF-β1 ($P = .002$, $P = .001$, $P = .001$, $P = .001$, respectively) and higher levels of E-cadherin than in group A ($P = .005$).

DISCUSSION

The results of the present study suggest that EW-7197 inhibited TGF-β1 signaling, leading to inhibition of granulation tissue formation caused by mechanical injury incurred by the bare metallic stent. The luminal diameter of the stented esophagus was significantly smaller in the vehicle-treated control group than in the drug-treated groups, indicating effective suppression of stent-induced granulation tissue formation by EW-7197. EW-7197 treatment significantly inhibited collagen accumulation in the drug-treated groups. Consistent with the gross findings, histologic examination demonstrated significantly less granulation tissue formation in the drug-treated groups, which correlated with esophagography findings. Consistently, Western blot analysis revealed that TGF-β1–induced phosphorylation of Smad3 was significantly inhibited in the drug-treated group. These results showed

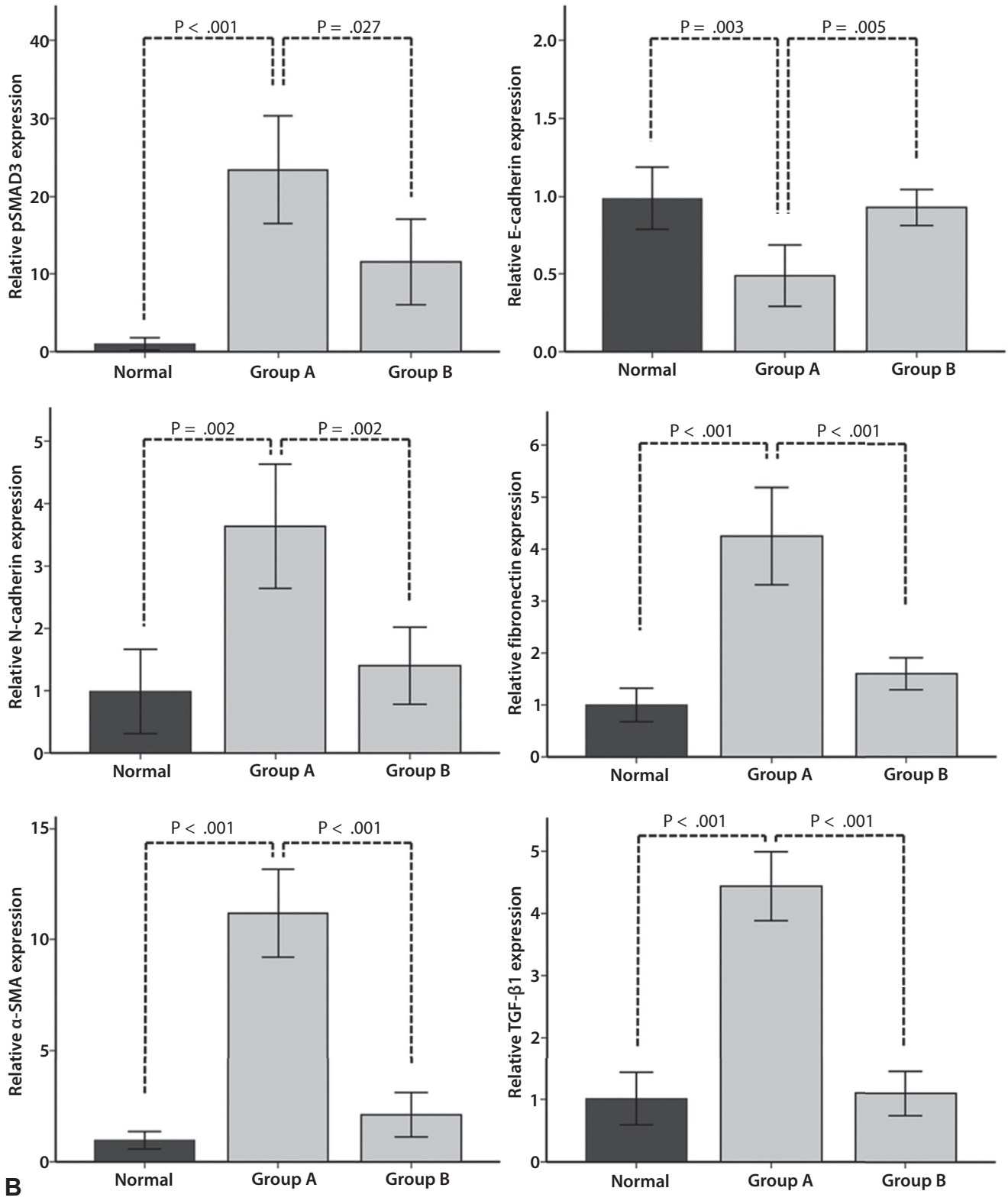

Figure 6. Continued.

that targeting TGF-β type I receptor kinase inhibitor by using EW-7197 selectively inhibited TGF-β/Smad signaling. Furthermore, EW-7197 reduced the levels of the mesenchymal markers N-cadherin, fibronectin, and α-smooth muscle actin and restored the level of the epithelial marker E-cadherin.

The TGF-β/SMAD pathway is a central mediator of wound healing and scaring processes. Therefore,

inhibition of TGF-β signaling by inhibiting ALK5 activity might negatively affect tissue healing. For example, Kim et al[9] reported that inguinal or abdominal herniation of the small bowel occurs at the injection site after intraperitoneal administration of an ALK5 inhibitor, IN-1233 and that hernia formation may have been caused by delayed wound healing and a reduction in granulation tissue formation. However, in the current study there were no adverse events after per-oral administration of EW-7197. EW-7197, which was recently introduced as an cancer immunotherapeutic/antifibrotic agent, is a highly potent, selective, and orally bioavailable ALK5 inhibitor.[16-18] According to the proposed therapeutic applications of ALK5 inhibitors and the favorable pharmacologic, pharmacokinetic, and toxicologic profiles of EW-7197 (IND 119528), a first-in-human dose-escalation study of EW-7197 in subjects with advanced-stage solid tumors is in progress in the United States (https://clinicaltrials.gov/ct2/show/NCT02160106). Our results demonstrated that EW-7197 effectively and safely suppressed granulation tissue formation after stent placement in the rat esophagus.

TGF-β/SMAD signaling stimulates most processes of fibrosis and tissue regeneration in association with the EMT and ECM synthesis and is a major profibrotic factor.[22-25] We have demonstrated for the first time that an ALK5 inhibitor suppressed granulation tissue formation by inhibiting TGF-β1/SMAD3-induced EMT and ECM synthesis. The EMT is associated with dramatic changes in ECM composition and attachment that act together to alter cell morphology.[26] The EMT induces dramatic reorganization of the ECM, because many EMT-inducing factors upregulate the expression of ECM proteins. Here we showed that the level of E-cadherin, which mediates epithelial cell–cell interactions, was higher in the drug-treated group than in the vehicle-treated control group. Consistently, the level of N-cadherin, which mediates myofibroblast cell–cell interactions, was lower in the drug-treated group than in the vehicle-treated control group. Moreover, the levels of α-smooth muscle actin, which is a myofibroblast marker, and fibronectin, which is a glycoprotein component of the ECM, were lower in the drug-treated group than in the vehicle-treated control group. Our results strongly suggest that EW-7197 inhibits granulation tissue formation caused by bare metallic stent placement by blocking EMT and ECM synthesis in a rat esophageal model.

EW-7197 may also have potential value as a drug to prevent other esophageal stricture formations. The development of post–lye-induced, peptic, anastomotic esophageal strictures are all involved with increased expression of TGF-β1.[27-29] Thus, we assume that EW-7197 could be used as an antistructuring drug. However, EW-7197 may be limited to acute postoperative applications and further emphasize the importance of identifying more selective strategies to modify the wound-healing and scaring processes that might be more useful for the treatment of esophageal strictures.[30] Although several treatment protocols have been devised, the benefit and standardization of these treatments are still controversial.[31]

The rebound effect occurs after discontinuation of numerous classes of drugs. In our study the results of EW-7197 withdrawal 4 weeks after stent placement were obtained to evaluate the rebound effect. There were no differences in results between groups C and D, including esophagographic and histopathologic findings. Gratifyingly, the patency of the stent was maintained for 8 weeks in group C after withdrawal of EW-7197. Wound healing after mechanical injury is divided into inflammatory, fibroblastic, and granulation phases within approximately 4 weeks.[19,20] Early on, fibroblast and epithelial cells migrate to the wound site where they form highly vascular granulation tissue. Our results showed no rebound effects after EW-7197 withdrawal after 4 weeks; thus, long-term use of this drug may not be necessary. Nonetheless, further studies, including long-term follow-up, are required to confirm our findings.

Advances in stent technology have contributed to high success rate of stent placement, and recent attention is focused on long-term preservation of stent patency. Stent-induced stenosis is caused by granulation tissue formation and fibrosis, and treatment in vitro and in vivo with dexamethasone, paclitaxel, gemcitabine, or irradiation applied is used to inhibit stent obstruction in nonvascular luminal organs.[9,10,25,26,32-35] Unfortunately, current therapies are insufficient. Our present study demonstrates the potential of EW-7197 to reduce granulation tissue formation in a rat esophageal model by acting as a selective ALK5 inhibitor. More recent stent innovations include local drug delivery via drug-eluting stents to treat nonvascular diseases.[10,26,32-35] As a next step, stents eluting EW-7197 should be developed with the expectation of enhanced safety and a more effective and controlled dose than per-oral administration. Delivery of this drug via a stent potentially allows for a localized and sustained effect on stent-induced stenosis. Furthermore, the combination of the pharmacologic effects of EW-7197 with the mechanical advantages of a covered stent could allow its application to benign strictures in nonvascular luminal organs after all other treatment options are exhausted.

There are some limitations to our study. First, we did not evaluate the toxicity and side effects of EW-7197, although this is the goal of the study (NCT02160106) described above. Second, only a few representative markers of the ECM and EMT were evaluated in this study. Third, it is necessary to determine the exact time to discontinue drug administration in a further study. In conclusion, EW-7197 is effective and safe for the suppression of granulation tissue formation after stent placement in a rat esophageal model and possesses strong potential as an antifibrotic agent via its ability to inhibit TGF-β signaling.

REFERENCES

1. Boyce HW Jr. Stents for palliation of dysphagia due to esophageal cancer. N Engl J Med 1993;329:1345-6.
2. Song HY, Do YS, Han YM, et al. Covered, expandable esophageal metallic stent tubes: experiences in 119 patients. Radiology 1994;193:689-95.
3. Ross WA, Alkassab F, Lynch PM, et al. Evolving role of self-expanding metal stents in the treatment of malignant dysphagia and fistulas. Gastrointest Endosc 2007;65:70-6.
4. Shin JH, Song HY, Ko GY, et al. Esophagorespiratory fistula: long-term results of palliative treatment with covered expandable metallic stents in 61 patients. Radiology 2004;232:252-9.
5. Evrard S, Le Moine O, Lazaraki G, et al. Self-expanding plastic stents for benign esophageal lesions. Gastrointest Endosc 2004;60:894-900.
6. Song HY, Park SI, Do YS, et al. Expandable metallic stent placement in patients with benign esophageal strictures: results of long-term follow-up. Radiology 1997;203:131-6.
7. Kim JH, Song HY, Choi EK, et al. Temporary metallic stent placement in the treatment of refractory benign esophageal strictures: results and factors associated with outcome in 55 patients. Eur Radiol 2009;19:384-90.
8. Holm AN, de la Mora Levy JG, Gostout CJ, et al. Self-expanding plastic stents in treatment of benign esophageal conditions. Gastrointest Endosc 2008;67:20-5.
9. Kim JH, Song HY, Park JH, et al. IN-1233, an ALK-5 inhibitor: prevention of granulation tissue formation after bare metallic stent placement in a rat urethral model. Radiology 2010;255:75-82.
10. Kim EY, Song HY, Kim JH, et al. IN-1233-eluting covered metallic stent to prevent hyperplasia: experimental study in a rabbit esophageal model. Radiology 2013;267:396-404.
11. Taylor MA, Parvani JG, Schiemann WP. The pathophysiology of epithelial–mesenchymal transition induced by transforming growth factor-β in normal and malignant mammary epithelial cells. J Mammary Gland Biol Neoplasia 2010;15:169-90.
12. Shi Y, Massague J. Mechanisms of TGF-β signaling from cell membrane to the nucleus. Cell 2003;113:685-700.
13. Massague J. How cells read TGF-β signals. Nat Rev Mol Cell Biol 2000;1:169-78.
14. Lindley LE, Briegel KJ. Molecular characterization of TGFb-induced epithelial-mesenchymal transition in normal finite lifespan human mammary epithelial cells. Biochem Biophys Res Commun 2010;399:659-64.
15. Leask A, Abraham DJ. TGF-β signaling and the fibrotic response. FASEB J 2004;18:816-27.
16. Park SA, Kim MJ, Park SY, et al. EW-7197 inhibits hepatic, renal, and pulmonary fibrosis by blocking TGF-β/Smad and ROS signaling. Cell Mol Life Sci 2015;72:2023-39.
17. Jin CH, Krishnaiah M, Sreenu D, et al. Discovery of *N*-((4-([1,2,4]triazolo[1,5-a]pyridin-6-yl)-5-(6-methylpyridin-2-yl)-1H-imidazol-2-yl)methyl)-2-fluoroaniline (EW-7197): a highly potent, selective, and orally bioavailable inhibitor of TGF-β type I receptor kinase as cancer immunotherapeutic/antifibrotic agent. J Med Chem 2014;57:4213-38.
18. Son JY, Park SY, Kim SJ, et al. EW-7197, a novel ALK-5 kinase inhibitor, potently inhibits breast to lung metastasis. Mol Cancer Ther 2014;13:1704-16.
19. Kim EY, Shin JH, Jung YY, et al. A rat esophageal model to investigate stent-induced tissue hyperplasia. J Vasc Interv Radiol 2010;21:1287-91.
20. Park JH, Kim JH, Kim EY, et al. Bioreducible polymer-delivered siRNA targeting MMP-9: suppression of granulation tissue formation after bare metallic stent placement in a rat urethral model. Radiology 2014;271:87-95.
21. Koh RY, Lim CL, Uhal BD, et al. Inhibition of transforming growth factor-beta via the activin receptor-like kinase-5 inhibitor attenuates pulmonary fibrosis. Mol Med Rep 2015;11:3808-13.
22. Ohnuma-Koyama A, Yoshida T, Tajima-Horiuchi H, et al. Didecyldimethylammonium chloride induces pulmonary fibrosis in association with TGF-beta signaling in mice. Exp Toxicol Pathol 2013;65:1003-9.
23. de Gouville AC, Boullay V, Krysa G, et al. Inhibition of TGF-beta signaling by an ALK5 inhibitor protects rats from dimethylnitrosamine-induced liver fibrosis. Br J Pharmacol 2005;145:166-77.
24. Park JH, Choi KC, Lee SW, et al. SKI2162, an inhibitor of the TGF-β type I receptor (ALK5), inhibits radiation-induced fibrosis in mice. Oncotarget 2015;28:4171-9.
25. Prud'homme GJ. Pathobiology of transforming growth factor beta in cancer, fibrosis and immunologic disease, and therapeutic considerations. Lab Invest 2007;87:1077-91.
26. Shin JH, Song HY, Seo TS, et al. Influence of a dexamethasone-eluting covered stent on tissue reaction: an experimental study in a canine bronchial model. Eur Radiol 2005;15:1241-9.
27. Zhou JH, Jiang YG, Wang RW, et al. Prevention of stricture development after corrosive esophageal burn with a modified esophageal stent in dogs. J Gen Thoracic Surg 2008;136:1336-42.
28. Shawn SG, David DO, James DK, et al. Esophageal strictures refractory to endoscopic dilatation. Gastrointest Surg 2015;28:13-22.
29. Zhao H, Zhao L, Zhou Z, et al. The roles of connective tissue growth factor in the development of anastomotic esophageal strictures. Arch Med Sci 2015;11:770-8.
30. Kane CJ, Hebda PA, Mansbridge JN, et al. Direct evidence for spatial and temporal regulation of transforming growth factor beta 1 expression during cutaneous wound healing. Cell Physiol 1991;148:157-73.
31. Orozco-Perez J, Aguirre-Jauregui O, Salazar-Montes AM, et al. Pirfenidone prevents rat esophageal stricture formation. J Surg Res 2015;194:558-64.
32. Shin JH, Song HY, Choi CG, et al. Tissue hyperplasia: influence of a paclitaxel-eluting covered stent—preliminary study in a canine urethral model. Radiology 2005;234:438-44.
33. Moo S, Yang SG, Na K. An acetylated polysaccharide-PTFE membrane-covered stent for the delivery of gemcitabine for treatment of gastrointestinal cancer and related stenosis. Biomaterials 2011;32:3603-10.
34. Kim SY, Kim M, Kim MK, et al. Paclitaxel-eluting nanofiber-covered self-expanding nonvascular stent for palliative chemotherapy of gastrointestinal cancer and its related stenosis. Biomed Microdev 2014;16:897-904.
35. Shaikh M, Kichenadasse G, Choudhury NR, et al. Non-vascular drug eluting stents as localized controlled drug delivery platform: preclinical and clinical experience. J Control Release 2013;172:105-17.